Journal of ELECTRONIC MATERIALS
DOI: 10.1007/s11664-012-1960-6
© 2012 TMS

$LaAlO_3/SrTiO_3$ Epitaxial Heterostructures by Atomic Layer Deposition

NICK M. SBROCKEY,[1,3] MICHAEL LUONG,[1] ERIC M. GALLO,[2] JENNIFER D. SLOPPY,[2] GUANNAN CHEN,[2] CHRISTOPHER R. WINKLER,[2] STEPHANIE H. JOHNSON,[2] MITRA L. TAHERI,[2] GARY S. TOMPA,[1] and JONATHAN E. SPANIER[2]

1.—Structured Materials Industries, Inc., 201 Circle Drive North, Unit #102, Piscataway, NJ 08854, USA. 2.—Department of Materials Science and Engineering, Drexel University, Philadelphia, PA 19104, USA. 3.—e-mail: sbrockey@optonline.net

Thin films of $LaAlO_3$ were deposited on TiO_2-terminated (100) $SrTiO_3$ crystals by atomic layer deposition (ALD), using tris(iso-propylcyclopentadienyl)lanthanum and trimethyl aluminum precursors. Water was used as the oxidizer. The film composition was shown to be controlled by the ratio of La/Al precursor pulses during ALD, with near-stoichiometric $LaAlO_3$ resulting at precursor pulse ratios of 4/1 to 5/1. Films near the stoichiometric $LaAlO_3$ composition were shown to crystallize on subsequent annealing to form epitaxial $LaAlO_3/SrTiO_3$ heterostructures. Electrical characterization of these structures was done by two-terminal direct-current (DC) current–voltage scans at room temperature and under high-vacuum conditions. The results show electrical conductivity for the ALD-deposited epitaxial $LaAlO_3/SrTiO_3$ heterostructures, which turns on for thickness above four unit cells for the $LaAlO_3$ film.

Key words: $LaAlO_3$, $SrTiO_3$, heterostructures, ALD, epitaxial

INTRODUCTION

Recently, there has been considerable interest in the structure and electrical properties of oxide heterojunctions. The most widely studied system is $LaAlO_3$ on $SrTiO_3$.[1–8] This interest was sparked by the observation of electrical conductivity near the $LaAlO_3/SrTiO_3$ interface, which was shown to turn on at a critical film thickness of the $LaAlO_3$ film.[1] For $LaAlO_3$ films near this critical thickness, the high-conductivity layer can be switched from a metallic state to an insulating state by an applied gate voltage.[2] To date, most of the $LaAlO_3/SrTiO_3$ heterostructures investigated have been prepared by pulsed laser deposition (PLD). For ultimate production of devices based on oxide heterostructures, deposition of the films by atomic layer deposition (ALD) provides several significant advantages, including uniform deposition over large-area substrates, conformal deposition over device topography, and compatibility with standard microelectronic fabrication. ALD also provides greater flexibility to produce oxide heterostructures with a wide range of composition profiles. This work set out to demonstrate an ALD process to fabricate epitaxial $LaAlO_3/SrTiO_3$ heterostructures.

EXPERIMENTAL PROCEDURES

Two types of substrates were used in this investigation: (100) silicon and (100) $SrTiO_3$ single crystals. The $SrTiO_3$ crystals were hydroxylated, etched, and annealed to result in a TiO_2-terminated surface.[9,10] Each TiO_2-terminated $SrTiO_3$ substrate was cleaned in acetone, methanol, and deionized water, then dried in a nitrogen jet, prior to loading into the ALD reactor. Each silicon substrate was given a similar cleaning, then etched in 10% HF prior to loading into the ALD reactor. The ALD precursors were trimethyl aluminum (TMA) (Strem 98%) and tris(iso-propylcyclopentadienyl)lanthanum, La(i-PrCpd)$_3$ (Strem 99.9%). Water was used as the oxidizer. The TMA and water sources were

(Received July 25, 2011; accepted January 24, 2012)

Published online: 24 February 2012

maintained at room temperature. The La(i-PrCpd)$_3$ source was maintained at 150°C, with all downstream gas lines from the La(i-PrCpd)$_3$ source maintained at 180°C. The substrate temperature in the ALD reactor was 300°C. Ultrahigh-purity argon was used as the purge gas. After deposition, each sample was annealed at 900°C in air for 60 min.

For $La_xAl_{1-x}O_3$ films deposited on $SrTiO_3$ substrates, composition and thickness were determined by Rutherford backscattering spectroscopy (RBS). Structural characterization was done by x-ray diffraction (XRD) and transmission electron microscopy (TEM). For $La_xAl_{1-x}O_3$ and Al_2O_3 films deposited on silicon substrates, thickness was determined by optical reflectance spectroscopy using the known optical constants for Al_2O_3. We first established an ALD process for Al_2O_3, using TMA + water on silicon substrates. We next added the La(i-PrCpd)$_3$ + water steps. Initial investigation of $La_xAl_{1-x}O_3$ deposition was done on silicon substrates, to determine the effects of ALD parameters such as pulse length and purge times. We next deposited $La_xAl_{1-x}O_3$ films on TiO_2-terminated $SrTiO_3$ substrates, systematically varying the ratio of La/Al precursor pulses. We prepared relatively thick samples (approximately 40 nm to 140 nm) for structure and composition analysis.

We also prepared thin samples (up to approximately eight unit cell thickness) of near-stoichiometric $LaAlO_3$ films on TiO_2-terminated $SrTiO_3$ substrates for electrical characterization. Electrical contacts were patterned on the samples by photolithography and lift-off. The metallization consisted of approximately 5 nm Ti and 100 nm Au. The contact areas were 100 μm × 100 μm and 150 μm × 150 μm squares, with 40 μm, 20 μm, and 10 μm distances between squares. Two-terminal DC current–voltage (I–V) traces were collected at 300 K, under a vacuum of 10^{-6} Torr. For comparison, I–V traces were also collected for a similarly patterned and contacted uncoated TiO_2-terminated $SrTiO_3$ substrate.

RESULTS

For ALD of Al_2O_3, we observed an average growth rate of 0.126 ± 0.011 nm/cycle, which was independent of the pulse length for either TMA or water. These results are consistent with well-documented process technology for ALD of Al_2O_3.[11,12] For ALD of $La_xAl_{1-x}O_3$, the deposition rate was found to increase significantly with the La(i-PrCpd)$_3$ pulse length, as shown in Fig. 1. We found this to be true even for long argon purge times (up to 120 s) after the La(i-PrCpd)$_3$ pulse. With both the La and Al precursor pulse lengths kept constant at 1 s, film concentration was easily controlled by the number of La precursor pulses relative to the number of Al precursor pulses. Figure 2 shows the $La_xAl_{1-x}O_3$ film composition as a function of the La/Al precursor pulse ratio. Stoichiometric $LaAlO_3$ resulted at precursor pulse ratios between 4/1 and 5/1. Figure 3 shows the $La_xAl_{1-x}O_3$ film growth rate (as determined by RBS) as a function of the La/Al precursor pulse ratio. For stoichiometric $LaAlO_3$, the observed growth rate is about 1.7 nm/cycle.

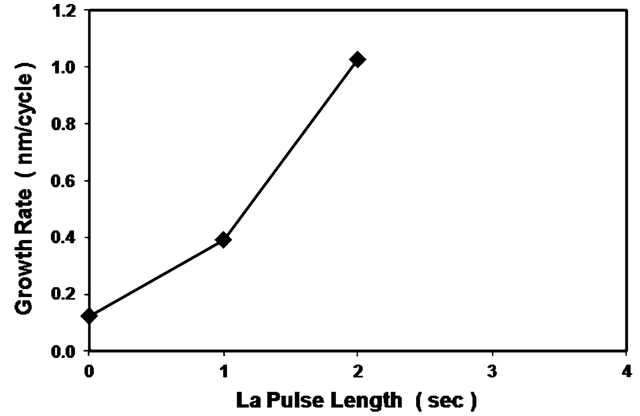

Fig. 1. Measured growth rate for $La_xAl_{1-x}O_3$ film deposition on silicon, as a function of the La precursor pulse length. The zero pulse length data point is the average growth rate observed for ALD of Al_2O_3. Film thickness was determined by optical reflectance spectroscopy.

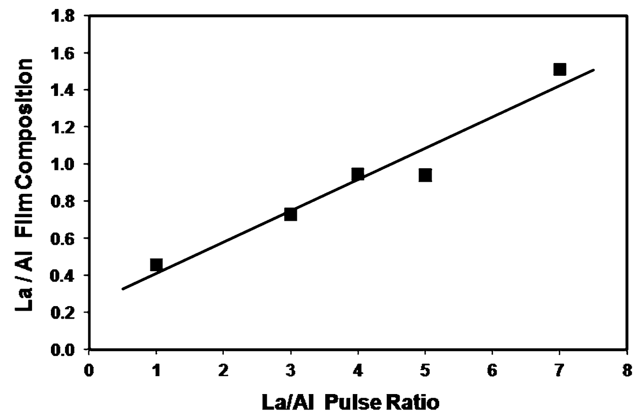

Fig. 2. $La_xAl_{1-x}O_3$ film composition, as a function of the ratio of La to Al precursor pulses during ALD on TiO_2-terminated $SrTiO_3$ substrates.

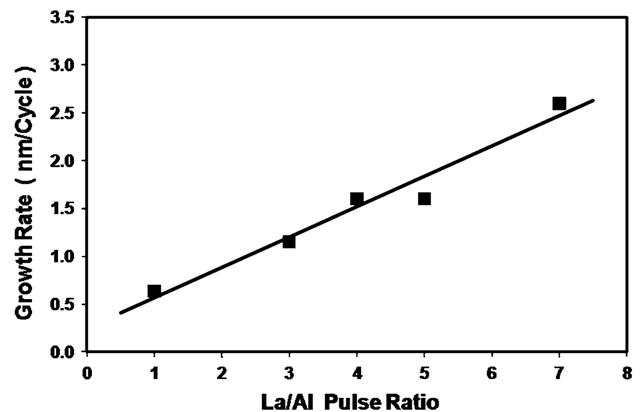

Fig. 3. $La_xAl_{1-x}O_3$ film deposition rate, as a function of the ratio of La to Al precursor pulses during ALD on TiO_2-terminated $SrTiO_3$ substrates.

To evaluate film structure and crystallinity, relatively thick $LaAlO_3$ films were deposited on TiO_2-terminated $SrTiO_3$, using a La/Al precursor pulse ratio of 5/1. No XRD peaks were observed for the as-deposited films. After annealing at 900°C, crystalline (h00) $LaAlO_3$ peaks were observed, as shown in Fig. 4, and no evidence of any other orientations or phases. High-resolution TEM and selected-area electron diffraction was done on representative cross-sections of $LaAlO_3/SrTiO_3$ heterostructures. Figure 5a demonstrates excellent crystallinity of the annealed $LaAlO_3$ film. Close inspection of the image reveals an interface that is coherent at the atomic level but strained. The fast Fourier transform of a HR-TEM image of the interface (Fig. 5b) and the diffraction pattern (Fig. 5c) indicate that $LaAlO_3$ forms (100) planes coincident on the (100) planes of the $SrTiO_3$ substrate.

Electrical conductivity for the epitaxial $LaAlO_3/SrTiO_3$ heterostructures was determined by two-terminal I–V scans using samples with rectangular patterned metal contacts on the surface of the $LaAlO_3$ film. Figure 6 shows a representative I–V scan. Electrical characterization results for the ALD-deposited $LaAlO_3/SrTiO_3$ heterostructures and the uncoated $SrTiO_3$ substrate are summarized in Table I. These results were obtained under high-vacuum conditions, to minimize any effects of adsorbed water vapor and other atmospheric contaminants on the conductivity measurements. The $LaAlO_3$ film thickness listed in Table I was estimated from the measured deposition rate data of Fig. 3. In order to compare conductivity between different samples, Table I lists the DC current observed at an applied potential of 10 V. The results show negligible conductivity for the uncoated $SrTiO_3$ substrate and for the $LaAlO_3/SrTiO_3$

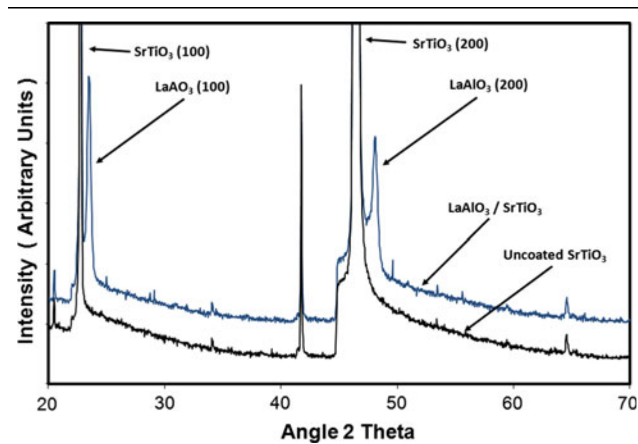

Fig. 4. X-ray diffraction results for a $LaAlO_3$ film deposited on TiO_2-terminated $SrTiO_3$ by ALD at La/Al precursor pulse ratio of 5/1 and a total of 60 ALD cycles. Also shown are results for an uncoated $SrTiO_3$ substrate.

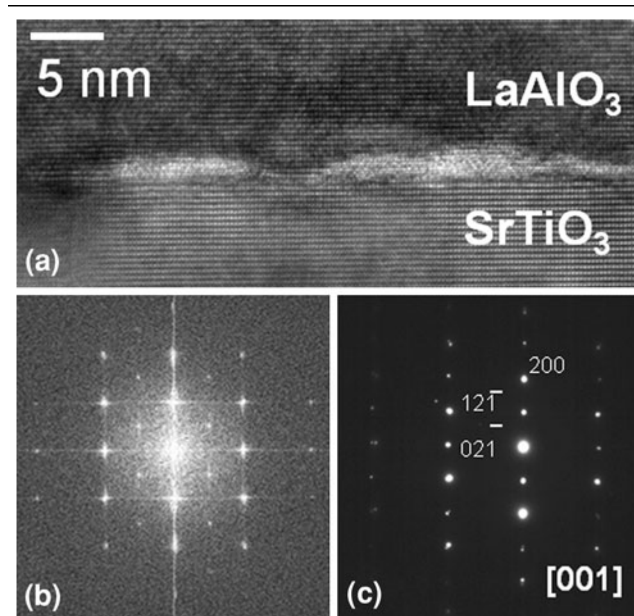

Fig. 5. (a) HR-TEM image of the interface between $SrTiO_3$ and $LaAlO_3$ demonstrating crystallinity of the $LaAlO_3$ and coherency of the interface. (b) Fast Fourier transform of a HR-TEM image of the $LaAlO_3$ film and $SrTiO_3$ substrate. (c) Selected-area diffraction pattern of the $LaAlO_3$ film and $SrTiO_3$ substrate along the [001] zone axis.

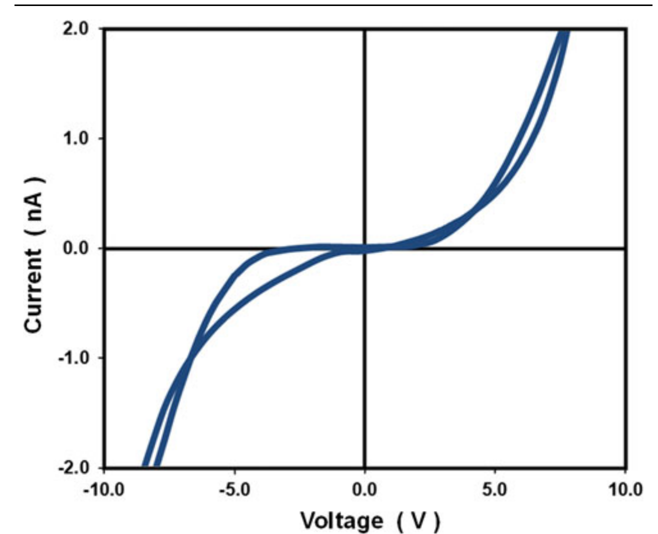

Fig. 6. Two-terminal current–voltage scan for an eight unit cell thickness $LaAlO_3$ film deposited on TiO_2-terminated (100) $SrTiO_3$ and annealed at 900°C. Results were obtained at 300 K under vacuum of 10^{-6} Torr.

Table I. Results of electrical characterization for $LaAlO_3/SrTiO_3$ heterostructures prepared by ALD

La/Al Precursor Pulse Ratio	Thickness (Unit Cells)	I–V Current (pA) @ 10 V
Uncoated $SrTiO_3$ substrate		15
4/1	4	150
4/1	8	4000

heterostructure with four unit cell thickness of $LaAlO_3$ film. Electrical conductivity is shown to increase significantly when the $LaAlO_3$ film thickness increases from four unit cells to eight unit cells.

DISCUSSION

This study found Al incorporation in Al_2O_3 films using TMA and water to be self-limiting, as expected for ALD of Al_2O_3. La incorporation during ALD of $La_xAl_{1-x}O_3$ was not self-limiting, as the data of Fig. 1 indicate. Adding the La(*i*-PrCpd)$_3$ plus water step appears to also destroy the self-limiting nature of Al incorporation during ALD of $La_xAl_{1-x}O_3$ films. Note that the observed deposition rate for stoichiometric $LaAlO_3$ was over 10 times greater than that for ALD-deposited Al_2O_3. If Al incorporation were not affected by the presence of La(*i*-PrCpd)$_3$, we would expect the deposition rate of stoichiometric $LaAlO_3$ to be about two times that of Al_2O_3.

There are three general categories of precursors typically used for ALD of oxides: (1) precursors with metal–oxygen bonds, such as alkoxides and β-diketonates, (2) precursors with metal–ligand bonds, such as alkyls and cyclopentadienyls, and (3) precursors with metal–nitrogen bonds, such as alkylamides and amidinates. A common precursor for chemical vapor deposition (CVD) of oxides containing lanthanum is the β-diketonate tris (2,2,6,6-tetramethyl-3,5-heptanedionato)lanthanum or La(thd)$_3$. While ALD of La compounds using La(thd)$_3$ and water has been reported,[13] it is generally observed that a stronger oxidizer such as ozone is needed to break the metal–oxygen bonds at typical ALD temperatures.[14,15] ALD of La-bearing oxides has also been reported using cyclopentadienyls, including tris(cyclopentadienyl)lanthanum[16] and tris(*iso*-propylcyclopentadienyl)lanthanum.[17,18] In these cases, the weaker metal–ligand bonds are easier to break using water as the ALD oxidizer. ALD of La-bearing oxides has also been reported using amidinate precursors, including tris(*N*,*N*′-diisopropylacetamidinato)lanthanum[19] and tris (*N*,*N*′-diisopropylformamidinate)lanthanum.[20,21] The metal– nitrogen bonds in these precursors are relatively weak, and expected to react with water in a similar manner to the ALD oxidizer.

In the present study, we used precursors with metal–ligand bonds, including the alkyl TMA and the cyclopentadienyl La(*i*-PrCpd)$_3$. It has been reported that lanthanum hydroxide forms during ALD of lanthanum oxide using an amidinate precursor and water.[19] This lanthanum hydroxide continues to release water during deposition and ruins the self-limiting nature of the ALD process.[19] Since we expect the metal–ligand-type precursors to react with water in a similar manner to the metal–nitrogen-type precursors, this mechanism probably also affected La incorporation in our $La_xAl_{1-x}O_3$ films. It is likely that this excess water vapor also affected Al incorporation in our $La_xAl_{1-x}O_3$ films. The results of Fig. 3 indicate a growth rate of about four unit cells per ALD cycle for stoichiometric $LaAlO_3$. Therefore, the Al incorporation rate must also be increasing in order to maintain stoichiometry. In spite of this non-self-limiting nature for deposition of $La_xAl_{1-x}O_3$ using La(*i*-PrCpd)$_3$, TMA, and water, the composition was found to be easily controllable by the ratio of La/Al precursor pulses. It should be possible to further tune the $La_xAl_{1-x}O_3$ film composition by adjusting the precursor pulse lengths, or the precursor source temperatures.

Electrical conductivity was observed for our ALD-deposited $LaAlO_3/SrTiO_3$ heterostructures, turning on above four unit cell thickness for the $LaAlO_3$ film. This observation shows good agreement with results reported for similar structures prepared by PLD.[2] The original explanation was that conductivity for $LaAlO_3/SrTiO_3$ heterostructures was due to the formation of a two-dimensional electron gas at the interface, due to the polar discontinuity.[1] Recently, it has been proposed that oxygen vacancies play a role in the electrical conductivity for $LaAlO_3/SrTiO_3$ heterostructures,[22] and that conditions during PLD of the films affect oxygen vacancy concentration and thus the depth of the high-conductivity layer.[23] The present study does not identify the conduction mechanism for the ALD-prepared $LaAlO_3/SrTiO_3$ heterostructures. The fact that electrical conductivity follows the same trend with film thickness implies that the conduction mechanism is similar for the ALD- and PLD-deposited heterostructures. If oxygen vacancies play a role in electrical conduction for our ALD-deposited $LaAlO_3/SrTiO_3$ heterostructures, then the oxygen vacancy concentration is most likely fixed by the annealing conditions in this work, rather than by the deposition conditions.

In summary, an ALD process has been demonstrated for $La_xAl_{1-x}O_3$ films. The film composition was shown to be controlled by the ratio of La/Al precursor pulses during ALD, with near-stoichiometric $LaAlO_3$ resulting at precursor pulse ratios of 4/1 to 5/1. Films near the stoichiometric $LaAlO_3$ composition deposited on TiO_2-terminated (100) $SrTiO_3$ substrates were shown to crystallize on subsequent annealing to form epitaxial $LaAlO_3/SrTiO_3$ heterostructures. Two-terminal DC current–voltage scans at room temperature and under high-vacuum conditions show electrical conductivity for the ALD-deposited epitaxial $LaAlO_3/SrTiO_3$ heterostructures, which turns on at thickness above four unit cells for the $LaAlO_3$ film. The electrical characterization results follow the same trend with thickness as reported for PLD-deposited $LaAlO_3$ films deposited on TiO_2-terminated (100) $SrTiO_3$ substrates. Oxide heterostructures offer significant potential for novel electrical devices. ALD has many advantages for producing a wide variety of oxide heterostructures for continued research into their properties. Ultimately, ALD should provide a robust and economical route to fabricating nanodevices based on oxide heterostructures.

ACKNOWLEDGEMENTS

This work was funded by the AFOSR under Contracts FA9550-09-C-0163 and FA9550-10-C-0163. J.E.S. acknowledges additional support at Drexel from the ARO under W911NF-08-1-0067 and from the NSF under an MRI under DMR-0722845 and from the NTI/BFTP. TEM analysis was carried out at the Centralized Research Facility at Drexel University.

REFERENCES

1. A. Ohtomo and H.Y. Hwang, *Nature* 427, 423 (2004).
2. S. Thiel, G. Hammerl, A. Schmehl, C.W. Schneider, and J. Mannhart, *Science* 313, 1942 (2006).
3. M. Huijben, G. Rijnders, D.A. Blank, S. Bals, S. Van Aert, J. Verbeeck, G. Van Tendeloo, A. Brinkman, and H. Hilgenkamp, *Nat. Mater.* 5, 556 (2006).
4. N. Reyren, S. Thiel, A.D. Caviglia, L. Fitting Kourkoutis, G. Hammerl, C. Richter, C.W. Schneider, T. Kopp, A.-S. Rüetschi, D. Jaccard, M. Gabay, D.A. Muller, J.-M. Triscone, and J. Mannhart, *Science* 317, 1196 (2007).
5. S. Gariglio, N. Reyren, A.D. Caviglia, and J.-M. Triscone, *J. Phys.* 21, 164213 (2009).
6. J. Mannhart, D.H.A. Blank, H.Y. Hwang, A.J. Millis, and J.-M. Triscone, *MRS Bull.* 33, 1027 (2008).
7. J. Mannhart and D.G. Schlom, *Science* 327, 1607 (2010).
8. P. Irvin, Y. Ma, D.F. Bogorin, C. Cen, C.W. Bark, C.M. Folkman, C.-B. Eom, and J. Levy, *Nat. Photon.* 4, 849 (2010).
9. A. Fragneto, G.M. De Luca, R. Di Capua, U. Scotti di Uccio, M. Salluzzob, X. Torrelles, T.-L. Lee, and J. Zegenhagen, *Appl. Phys. Lett.* 91, 101910 (2007).
10. G. Koster, B.L. Kropman, G.J.H.M. Rijnders, D.H.A. Blank, and H. Rogalla, *Appl. Phys. Lett.* 73, 2920 (1998).
11. M.D. Groner, J.W. Elam, F.H. Fabreguette, and S.M. George, *Thin Solid Films* 413, 186 (2002).
12. M.D. Halls and K. Raghavachari, *J. Chem. Phys.* 118, 10221 (2003).
13. S.Y. Kim, H. Kwon, S.J. Jo, J.S. Ha, W.T. Park, D.K. Kang, and B.-H. Kim, *Appl. Phys. Lett.* 90, 103104 (2007).
14. M. Roeckerath, T. Heeg, J. Lopes, J. Schubert, S. Mantl, A. Besmehn, P. Myllymaki, and L. Niinisto, *Thin Solid Films* 517, 201 (2008).
15. M. Nieminen, T. Sajavaara, E. Rauhala, M. Putkonena, and L. Niinisto, *J. Mater Chem.* 11, 2340 (2001).
16. X.L. Li, D. Tsoutsou, G. Scarel, C. Wiemer, S.C. Capelli, S.N. Volkos, L. Lamagna, and M. Fanciulli, *J. Vac. Sci. Technol. A* 27, L1 (2009).
17. D. Tsoutsou, L. Lamagna, S.N. Volkos, A. Molle, S. Baldovino, S. Schamm, P.E. Coulon, and M. Fanciulli, *Appl. Phys. Lett.* 94, 053504 (2009).
18. J.M. Gaskell, A.C. Jones, H.C. Aspinall, S. Taylor, P. Taechakumput, P.R. Chalker, P.N. Heys, and R. Odedra, *Appl. Phys. Lett.* 91, 112912 (2007).
19. B.S. Lim, A. Rahtu, P. de Rouffignac, and R.G. Gordon, *Appl. Phys. Lett.* 84, 3957 (2004).
20. S. Abermann, O. Bethge, C. Henkel, and E. Bertagnolli, *Appl. Phys. Lett.* 94, 262904 (2009).
21. H. Wang, J.-J. Wang, R. Gordon, J.-S.M. Lehn, H. Li, D. Hong, and D.V. Shenaic, *Electrochem. Solid State Lett.* 12, G13 (2009).
22. M. Basletic, J.-L. Maurice, C. Carrétéro, G. Herranz, O. Copie, M. Bibes, É. Jacquet, K. Bouzehouane, S. Fusil, and A. Barthélémy, *Nat. Mater.* 7, 621 (2008).
23. G. Herranz, M. Basletic, M. Bibes, C. Carretero, E. Tafra, E. Jacquet, K. Bouzehouane, C. Deranlot, A. Hamzic, J.-M. Broto, A. Barthelemy, and A. Fert, *Phys. Rev. Lett.* 98, 216803 (2007).